MOLECULAR IMAGING AND BIOLOGY

Mol Imaging Biol (2019) 21:67–77
DOI: 10.1007/s11307-018-1209-8

Published Online: 1 June 2018

RESEARCH ARTICLE

An Innovation for Treating Orthotopic Pancreatic Cancer by Preoperative Screening and Imaging-Guided Surgery

Ziyu Han,[1,2,3,4] Wenting Shang,[2] Xiaoyuan Liang,[1,4] Hao Yan,[2] Min Hu,[1,4] Li Peng,[2] Hongmei Jiang,[2] Chihua Fang,[1,4] Kun Wang,[2] Jie Tian[2,3,5,6]

[1]*Department of Hepatobiliary Surgery, Zhujiang Hospital, Southern Medical University, Guangzhou, 510280, China*
[2]*CAS Key Laboratory of Molecular Imaging, the State Key Laboratory of Management and control for Complex Systems, Institute of Automation, Chinese Academy of Sciences, Beijing, 100190, China*
[3]*University of Chinese Academy of Sciences, Beijing, 100080, China*
[4]*Guangdong Provincial Clinical and Engineering Center of Digital Medicine, Guangzhou, 510280, China*
[5]*CAS Center for Excellence in Brain Science and Intelligence Technology, Institute of Automation, Chinese Academy of Sciences, Beijing, China*
[6]*CAS Key Laboratory of Molecular Imaging, Institute of Automation, Chinese Academy of Sciences, Zhongguancun East Road #95, Haidian Dist, Beijing, 100190, China*

Abstract

Purpose: Pancreatic cancer is still associated with a poor outcome and low patient quality of life, which are mainly attributed to the late detection and requirement of distal pancreatectomy with extended resection of pancreatic tumors. Therefore, novel strategies for early screening and precise tumor resection are urgently needed. In this study, we evaluated the feasibility of a low-density lipoprotein receptor (LDLR)-targeted small-molecule contrast agent (peptide-22-Cy7) for early screening with photoacoustic tomography and near-infrared (NIR) imaging as guided surgical navigation to achieve precise resection.

Procedure: Normal pancreatic cells (HPDE6-C7) and cancer cells (PANC-1) were respectively used in the *in vitro* targeting evaluations. The ability of peptide-22-Cy7 for preoperative *in vivo* pancreatic tumor detection was investigated in a mouse orthotopic pancreatic cancer model ($n = 10$) using photoacoustic tomography; 18 tumor-bearing mice were further divided into three groups for different treatments. After intravenous injection of peptide-22-Cy7, surgical navigation was conducted through laparotomy. Histopathological analysis was used to further confirm the tumor area and the state of surgical margins.

Results: Flow cytometry demonstrated that peptide-22 is highly specific to pancreatic cancer cells, with a fluorescence intensity of approximately 87.3 %. Orthotopic pancreatic tumors with a size of 4 mm could be accurately detected by photoacoustic tomography. Surgical navigation effectively achieved R0 resection and minimized the range of resection, which led to increased body weight of the mice following surgery.

Electronic supplementary material The online version of this article (https://doi.org/10.1007/s11307-018-1209-8) contains supplementary material, which is available to authorized users.

Correspondence to: Chihua Fang; *e-mail:* fangch_dr@163.com, Kun Wang; *e-mail:* kun.wang@ia.ac.cn, Jie Tian; *e-mail:* jie.tian@ia.ac.cn

Conclusion: Overall, our newly developed targeted contrast agent facilitated the accurate positioning and resection of pancreatic tumors. Photoacoustic tomography and optical imaging-guided surgical navigation may be a novel direction for improving the survival, quality of life, and disease management of pancreatic cancer patients.

Key words: Low-density lipoprotein receptor (LDLR), Photoacoustic imaging, Optical-guided surgery, Peptide-22

Introduction

Pancreatic cancer is an extremely devastating malignancy, and the increase in the mortality rate has essentially paralleled that of disease incidence [1]. Despite major improvements in the survival rate for most cancer types over the past three decades, the prognosis for pancreatic cancer has remained essentially the same over this period, with a 5-year survival rate less than 5 % and an approximately 6-month median survival rate following diagnosis [2]. This poor outcome is mainly due to the asymptomatic nature of the disease, in which symptoms generally manifest during the late stage of disease progression. Therefore, surgical resection remains the only essential curative option for pancreatic cancer. Approximately 20 % of patients who present with localized disease are eligible for surgical resection, and the median survival rate is only 25 % [3]. In addition to the late diagnosis, the poor outcomes for pancreatic cancer patients are also related to the lack of precise resection in surgery. Hence, greater efforts are urgently needed to find novel strategies that can improve early screening and precise tumor resection.

Before the onset of adverse symptoms, imaging during routine physical examination can serve as an important measure to promote the early screening of pancreatic cancer [4]. The detection of suspicious lesions in a physical examination contributes to the timely treatment of patients at a stage when the disease is still curable. Traditional preoperative imaging modalities of diagnosis include computed tomography, magnetic resonance imaging, ultrasonography, and positron emission computed tomography, which are widely available worldwide [5]. However, these imaging techniques are prone to certain shortcomings, including the inability to detect pancreatic cancers with high sensitivity and specificity, which have thus far hindered their application in early screening programs during physical examination. However, newly developed imaging techniques have been gaining more and more attention in the medical field. As compared with traditional imaging, photoacoustic imaging offers several important advantages such as high spatial resolution, reduced light scatter, low cost, lack of radiation, and easy operation procedures [6, 7]. Therefore, photoacoustic imaging is gaining popularity as a novel biomedical imaging modality, offering a new strategy for early screening that can improve the detection of the biological properties of the entire tumor, which can greatly facilitate therapeutic decisions.

As mentioned above, the critical problem contributing to long-term outcomes in pancreatic cancer is precise tumor resection. To achieve R0 resection, some surgeons advocate for extended resection, which is a more radical surgery that can lead to serious complications such as insulin-dependent diabetes mellitus, steatorrhea, and weight loss [8]. Intraoperative frozen sectioning is the conventional method of R0 resection but often requires additional surgeries due to time constraints in the initial operation [9]. One way to overcome these current deficiencies is to improve the tools for surgical navigation that could achieve more precise and guided resection. Optical-guided surgical navigation, as a high sensitivity technique, is an effective intraoperative tool for more precise tumor resection *via* injection of a fluorescent detection agent [10]. Such precision can allow for accurate removal of tumor tissues while retaining much more of the normal anatomy and physiological function to ultimately enhance patient outcomes and quality of life. However, current optical surgical navigation methods require improvement to reduce the rate of false-positive detection, which is mainly due to the absence of specific biological targets and optical contrast agents.

Low-density lipoprotein (LDL) is one of the routine factors assessed in blood tests during health examination since it is associated with lipoprotein metabolism [11, 12]. Indeed, reprogramming of lipid metabolism has been linked to the pathogenesis of rapidly proliferating malignancies, which is manifested by increased uptake of exogenous lipoproteins and expression of low-density lipoprotein receptor (LDLR) in a variety of tumor cells [13, 14]. Therefore, LDLR can be a potential biological target; however, vast validations are urgently needed before its clinical application. Although several of the targeting moieties derived from LDLR are less than ideal for imaging applications, peptide-22 shows good potential, which preferentially binds to LDLR over endogenous LDL and does not affect cholesterol homoeostasis [15, 16].

Thus, in this study, we aimed to develop a new modality for improving the early detection and precise tumor resection for pancreatic cancer using LDLR as a biological target. In particular, we synthesized peptide-22 conjugated to the fluorescent dye cyanine 7 (peptide-22-Cy7), which was used for preoperative targeted imaging and fluorescent imaging-guided surgical navigation in orthotopic mouse models of pancreatic cancer. These results can highlight LDLR as a new promising biological target for monitoring pancreatic

cancer progression and to achieve more precise surgical navigation in tumor resection.

Materials and Methods

The details of the experimental materials and methods are available in the electronic supplementary information.

Results

Characterization of Peptide-22-Dye Probe

Steady conjugation was first confirmed by mass spectroscopy (Fig. S1b, d), with values of 1812.34 ([M+H]+, calculated 1811.38) and 1403.445 ([M]+, calculated 1403.66) for peptide-22-Cy7 and peptide-22-FITC, respectively. The purity of each probe was about 95 % (Fig. S1e, f). Peptide-22-Cy7 had a strong absorption peak at 759 nm with an approximately 15 nm red shift compared to free Cy7, which further confirmed the successful conjugation (Fig. S2c). Moreover, the conjugation caused an approximately 6-nm red shift in the fluorescence emission peak of peptide-22-Cy7 as compared with that of free Cy7, with a peak at 788 nm under an excitation wavelength of 724 nm (Fig. S2a, b). Likewise, the peaks of excitation, emission, and absorption of peptide-22-FITC showed various red-shifted properties compared to those of FITC alone (Fig. S2d–f). This characterization confirmed the successful conjugation between peptide-22 and the fluorescent dyes.

In Fig. S3a, the fluorescence intensity rapidly increased along with increasing concentrations of peptide-22-Cy7 up to 30 nM, after which the intensity decreased with greater concentrations. A significant absorption band was acquired between 700 and 800 nm, as part of the NIR region, which revealed the potential photoacoustic imaging ability of the probe. The relative signal intensity increased with increasing concentrations of peptide-22-Cy7 from 0 to 240 nM (Fig. S3b), demonstrating a dose-dependent property to illustrate the intrinsic fluorescence/photoacoustic ability of peptide-22-Cy7.

Compared with free Cy7, peptide-22-Cy7 exhibited more stable absorbance when exposed to serum for 48 h (Fig. S3c). Although there was a slight decrease over time, these results demonstrated the long-term stability and good solubility of the probe without apparent aggregation *in vitro*.

Cellular Targeting Ability of Probe

The cytotoxicity of peptide-22-Cy7 was tested by MTT assay. Even at a high concentration (100 nM), the viability of the two cell lines was maintained at greater than 85 % with no adverse effects observed during the 24-h incubation period (Fig. 1a). The expression level of LDLR in PANC-1 cells was (0.41 ± 0.05), while it was (0.36 ± 0.03) in HPDE6-C7 normal cells (Fig. S4). Thus, LDLR displayed a higher expression level in pancreatic cancer cells compared with that in normal cells.

The internalization of peptide-22-FITC was further demonstrated with confocal laser scanning microscopy. Based on effective receptor-mediated endocytosis, large numbers of peptide-22-FITC were observed in PANC-1 cells, which were abundantly localized on the cytomembrane (Fig. 1b). In contrast, very little peptide-22-FITC entered HPDE6-C7 cells under the same condition. However, there was no significant difference in the uptake of free FITC between PANC-1 and HPDE6-C7 cells. The notable inhibition of free peptide led to a significant reduction in the fluorescent signal, which confirmed the strong and stable targeting ability between peptide-22 and LDLR. To further confirm this finding, the PANC-1 cells were magnified 100-fold and the cytoskeleton was stained with rhodamine-phalloidin, which allowed for clear detection of the uptake of peptide-22-FITC by PANC-1 cells (Fig. 1c).

Flow cytometry analysis was used to quantitatively confirm the imaging results. In Fig. 1d, the fluorescence signal of peptide-22-FITC-treated cells was higher than that of the other groups for both cell lines. In addition, a slight right shift was observed in the free FITC-treated groups as compared with control (untreated) groups due to the occasional uptake of small molecular dyes into the cells (Fig. 1d). In Fig. 1e, the fluorescence intensity of the peptide-22-FITC-treated group in PANC-1 cells reached 86.7 ± 1.27 %, which demonstrated a nearly 30 % increase as compared with that of peptide-22-FITC-treated HPDE6-C7 cells (54.6 ± 2.7 %; $P < 0.001$). The fluorescence intensity of the blocked group was reduced. These observations support that pancreatic cancer cells can uptake massive probes through peptide-22 targeting towards LDLR.

Distribution of Peptide-22-Cy7 In Vivo

The metabolism of the probes in orthotopic tumor-bearing mice was continuously monitored for 48 h. A strong fluorescence signal was spread over the entire body of the mice within 30 min p.i. From 4 to 48 h, the brightest fluorescence position was the same as that of tumor bioluminescent imaging (luciferase) in the peptide-22-Cy7 group, suggesting that the pancreatic tumor did not undergo metastasis *in situ* (Fig. 2a). These phenomena were not detected in the Cy7 group. Further quantitative analysis was performed by calculating the tumor-to-background ratio (TBR) with region-of-interest (ROI) image analysis. The maximum TBR value of the Peptide-22-Cy7 group was (3.72 ± 0.18) and occurred at 6 h, which was 1.7-fold greater than that of the Cy7 group (2.14 ± 0.25) (Fig. 2b). Therefore, the optimal cumulative time of peptide-22-Cy7 in the tumor area was 6 h. Overall, the metabolism of the two groups demonstrated significantly different TBR values over 48 h ($P < 0.05$). In particular, the TBR values in the peptide-22-

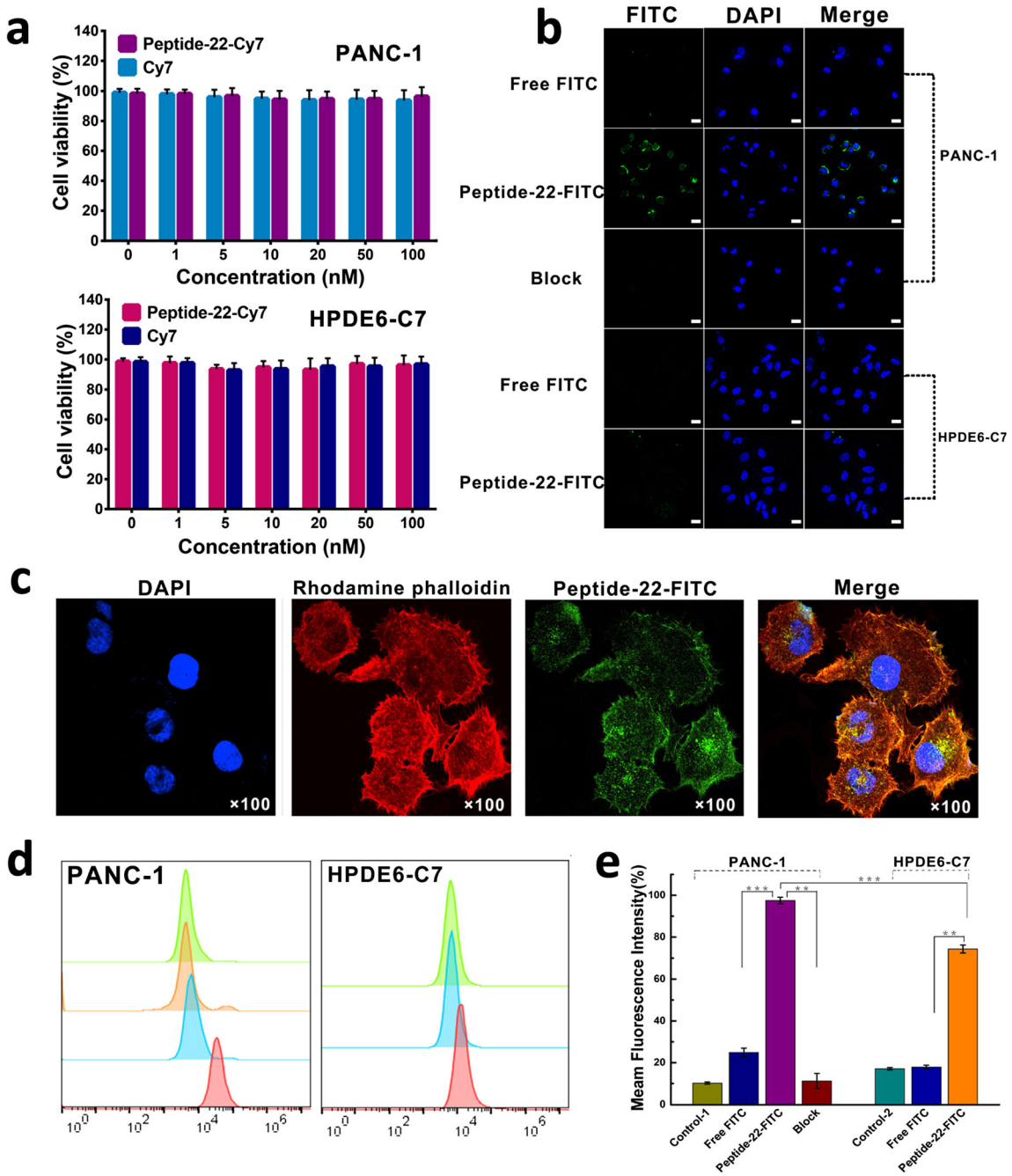

Fig. 1. Targeting ability of peptide-22-dye at the cellular level. **a** Cell viability of PANC-1 and HPDE6-C7. **b** Cellular uptake of peptide-22-FITC and free FITC in two cell lines. The block group was obtained with 1 mg/ml free peptide-22. (The bar represents 20 μm). **c** Confocal microscopy images (×100) of PANC-1 cell. **d e** Flow cytometry analyses (**d**: Green, control group; blue, free FITC group; red, Peptide-22-FITC group; orange, block group). A single asterisk indicates $P < 0.05$, double asterisks indicate $P < 0.01$, and triple asterisks indicate $P < 0.001$.

Cy7 group were much higher than those in the Cy7 group from 2 to 48 h.

The biodistribution of peptide-22-Cy7 was further examined in harvested tissues at 24 h p.i. Aside from the kidneys, the highest fluorescence intensities were detected in the tumors of the peptide-22-Cy7 group (Fig. 2c, d; $P < 0.001$).

The PANC-1 subcutaneous mouse model was established for a blocking study. In Fig. 2e, the fluorescence signal of tumor area was conspicuously inhibited in the blocked group between 30 min to 6 h ($P < 0.05$). By contrast, the control group showed a notable fluorescence signal at the tumor site and was confirmed by the TBR plot (Fig. 2f). However, with the metabolism of excess peptides, the circulating peptide-

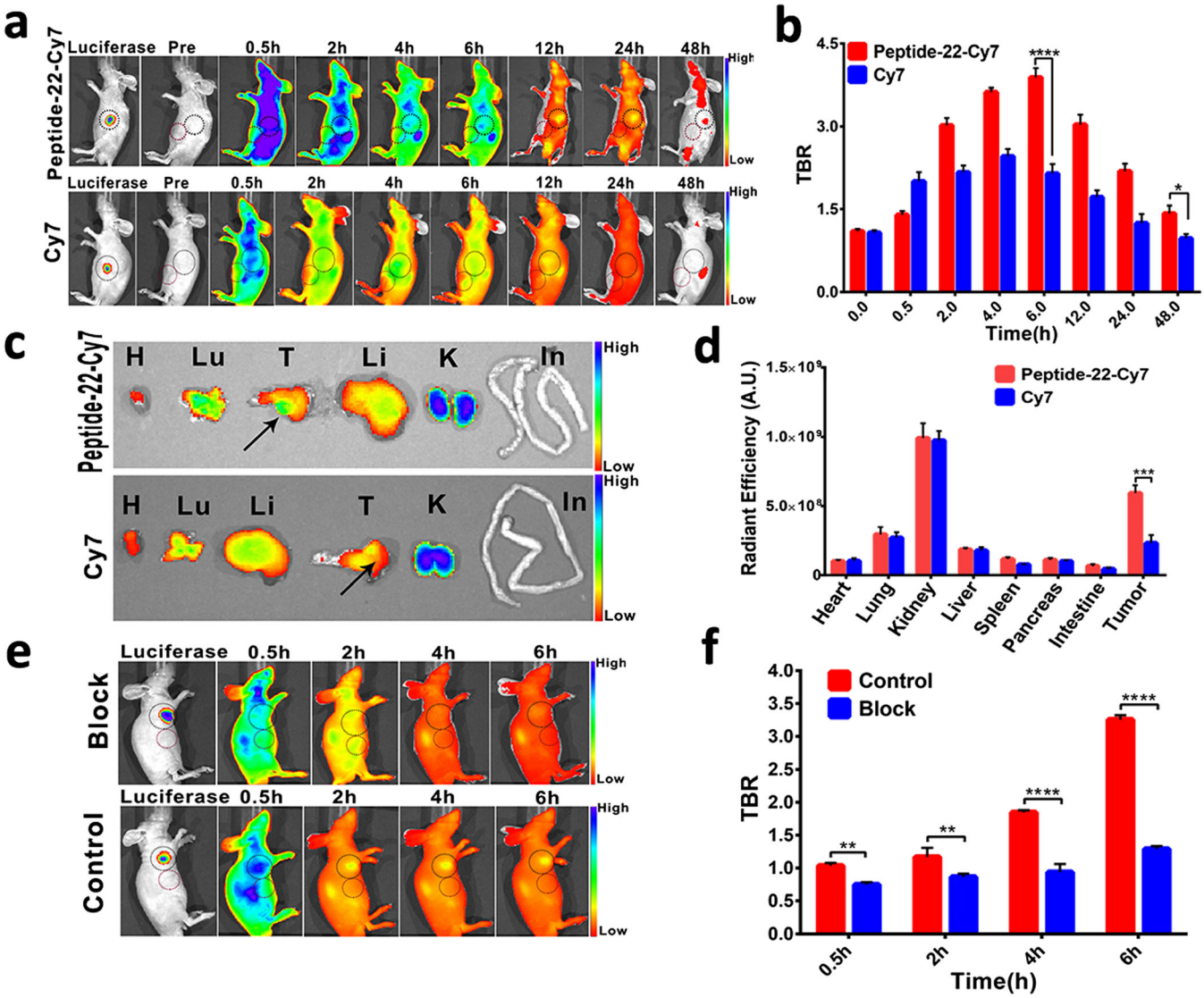

Fig. 2. Distribution of peptide-22-Cy7. **a** The biodistribution of peptide-22-Cy7 and free Cy7. **b** TBR profiles of two groups. **c***Ex vivo* imaging of tumor and major organs. **d** Related fluorescence intensity. **e** The block experiment of peptide-22-Cy7 in the subcutaneous mice model and **f** the corresponding TBR. (Large black dotted circles represent tumor area, and small red dotted circles represent background area; black arrows indicate tumor; H = heart; Lu = lung; Li = liver; K = kidney; In = intestine; T = tumor; S = spleen; $^{*}P < 0.05$, $^{**}P < 0.01$, $^{***}P < 0.001$, $^{****}P < 0.0001$).

22-Cy7 gradually targeted and accumulated at the tumor site so that the TBR values of the blocked group slowly increased over 6 h. Such specificity of peptide-22-Cy7 to LDLR would allow for clear distinction of the tumor from the surrounding tissue.

Microscopic Imaging of Tumor Areas

To further demonstrate the excellent targeted performance of the peptide-22-labeled probe, confocal laser endomicroscopy was applied to inspect differences in the distribution of peptide-22-dye between normal and tumor tissues at the microscopic level (Fig. 3). Prior to injection, a red dense arborized network was observed in the tumor tissues, which represented the microvessels of the tumor, demonstrating that the neovascularization of tumors was much more irregular than that of normal tissues. At 2 h p.i., peptide-22-FITC began to accumulate towards the tumor area through systemic delivery (Fig. 3a). In Fig. 3b, the main vascular region in the normal tissue was filled with green fluorescence of the probe without visible fluorescence diffusing at the periphery. However, the probe in the main vascular region of tumor could gradually target the surrounding tissue though the vascular pores. Finally, the tumor boundary showed large accumulation of probes on the tumor side but not on the normal side.

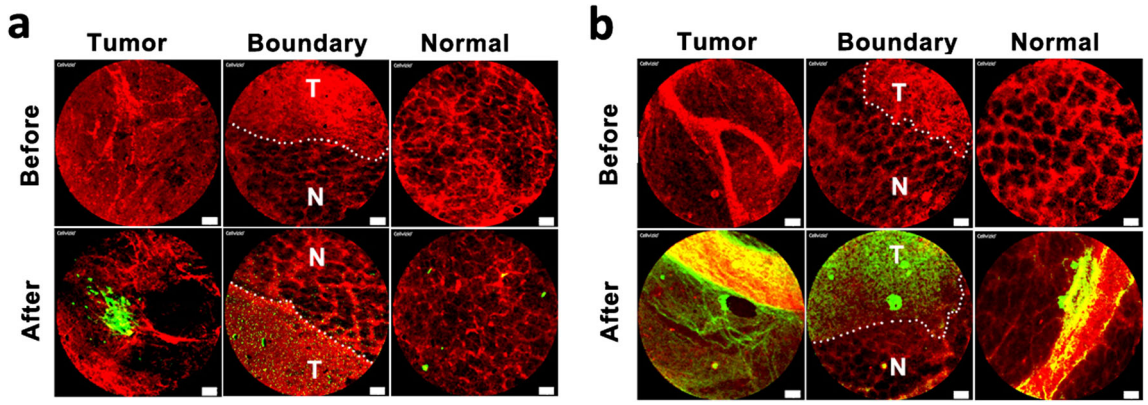

Fig. 3. Microscopic imaging of tumor tissue, tumor boundary, and adjacent normal pancreatic tissue. **a** The imaging of disorganized small blood vessels and **b** large main blood vessels in tissues. Both imaging were monitored at pre-injection and 2 h p.i. Scale bars = 50 μm. (Green: peptide-22-FITC; red: blood vessel staining with Evans blue; T = tumor; N = normal).

The microscopic biodistribution of peptide-22-FITC further verified the targeting ability of peptide-22, which would be beneficial for the preoperative detection of the tumor and surgical guidance.

Preoperative Detection by Photoacoustic Imaging

The orthotopic tumor was then examined by photoacoustic imaging preoperatively. In Fig. 4a, the photoacoustic signal of tumor area gradually increased over time. The optimal imaging time was 6 h confirming by quantitative analysis (Fig. 4b). As the laser intensity was only 70 Hz, the tumor was difficult to discriminate from the surrounding tissues. Therefore, three-dimensional conformation was applied to show the spatial distribution of probes at the tumor site at 6 h after injection (Fig. 4c). During the photoacoustic tomography imaging, the probe intensity values showed higher accumulation from 45 to 49 mm slices, which represent the portion of the tumor mass (Fig. 4d). After imaging for 48 h, the tumor-bearing pancreas was clearly separated and the tumor mass could be measured under white light (Fig. 4e). Based on the advantages of specific targeting, a 4-mm solid pancreatic tumor could be clearly defined and subsequently verified by pathological analysis. Therefore, peptide-22-Cy7 with photoacoustic imaging equipment can effectively detect orthotopic pancreatic cancer, which would facilitate the preoperative screening of diseased nude mice.

Fluorescence-Guided Surgical Resection

The orthotopic mouse model was successfully established without any distant metastasis confirmed by histopathological analysis (Fig. S5). As shown in Fig. 5a, compared with white light imaging, the fluorescence imaging yielded a brighter signal at the tumor site at 6 h p.i., which was more advantageous for the operator to distinguish the pancreatic tumor. In addition, visible fluorescent tissue residues were found following simulated primary surgical resection *in vivo* (Fig. 5b). Each fluorescence-positive location in the surgical bed was considered to be tumor-positive and was further removed until no fluorescence was visible. Moreover, the section of a rapidly frozen specimen could be further investigated by fluorescence imaging. According to the merged image, the fluorescence signal emerged at the tumor area (Fig. 5c), and the outlines of the tumor border were in agreement with results from pathological examinations. Histological examination of the surgical margin was negative, indicating the successful implementation of R0 resection by surgical navigation. Moreover, the pathological section indicated that the normal pancreatic tissue was only 0.25 mm thick. Thus, the surgical resection range could be minimized.

Therapeutic Effects of Surgical Navigation

The survival and body weight of mice were monitored to assess the quality of life after different surgeries (Fig. 6b). At 15 days post-treatment, the weights of mice in the control group gradually decreased and only two mice were still alive by 30 days. By contrast, the weights of mice that were subject to surgical navigation gradually increased and they were significantly heavier than the mice in surgery group, although one of the six mice was sacrificed on the third day because of a post-operative infection ($P > 0.05$). Although there was no obvious survival difference between the surgery and surgical navigation group (Fig. 6c), the mice in the surgical navigation group appeared to be healthier overall, which confirmed that precise resection with the imaging-guided system could improve the quality of life (Fig. S6). Although peptide-22-Cy7 proved to be safe at the cellular level, its short-term safety *in vivo* was further verified with histological analysis. In Fig. 6a, no notable tissue inflammation or toxicity effects of the major organs

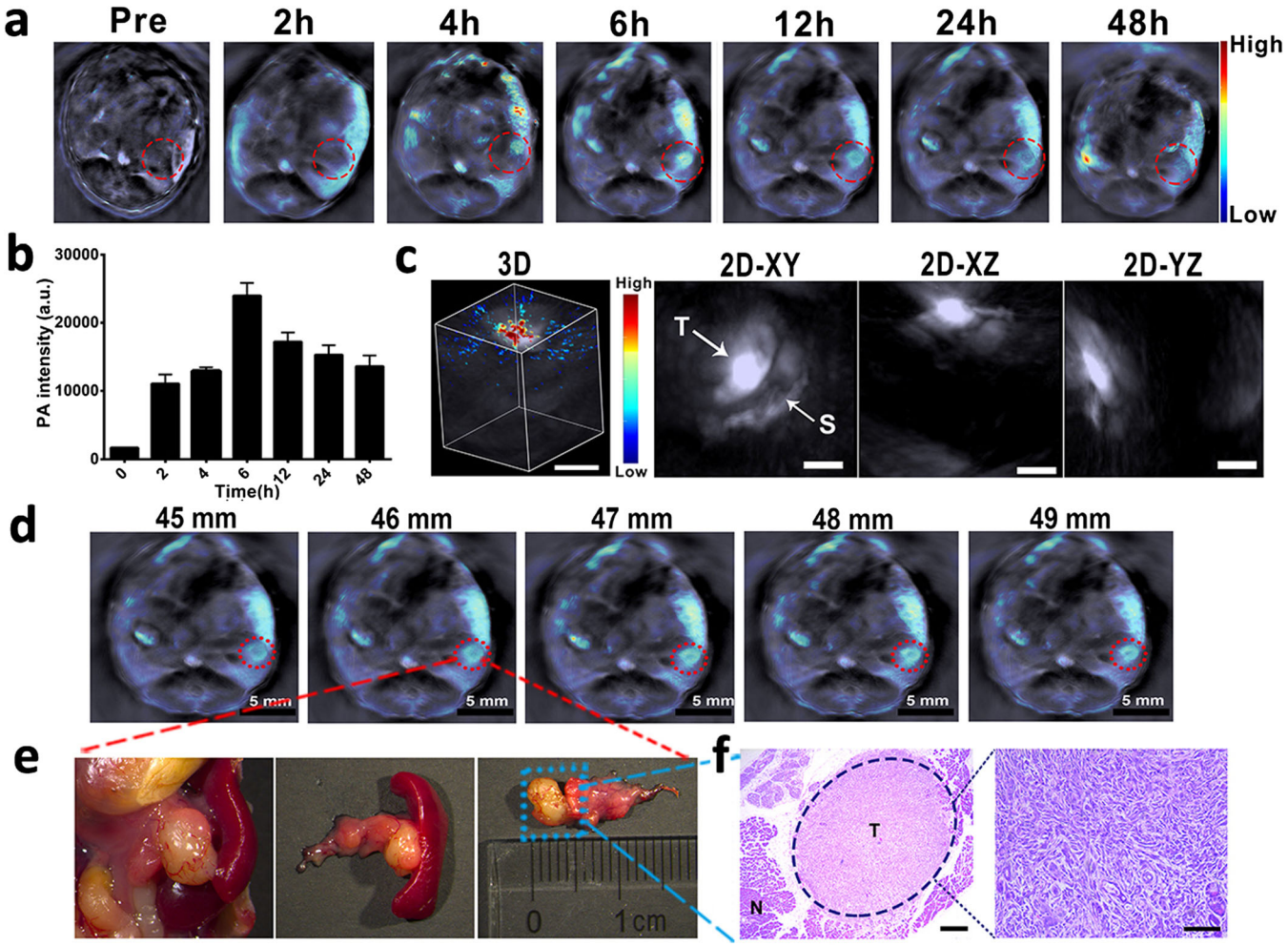

Fig. 4. **a** The cross-sectional photoacoustic images were aquired after injection of peptide-22-Cy7 and **b** quantitative analysis. **c** 3D conformation at 6 h p.i. (including *xy*, *xz*, *yz*). **d** The tumor was depicted from 45-mm frames to 49-mm frames and **e** was separated to investigate its anatomical position. **f** Histological examination of tumor (scale bar = 100 μm). (Red dotted circles and blue dotted square represent tumor area. T = tumor; N = normal).

were detected in the peptide-22-Cy7 group, with no differences observed from the control group.

Discussion

Image-guided surgical navigation is becoming increasingly important in operating rooms worldwide. Laparoscopic techniques are advantageous owing to the smaller incisions, reduced post-operative pain, fewer complications, and shorter hospital stays. However, these procedures lack tactile information, which is conducive to pancreatic cancer surgery. Furthermore, pancreatic tumors cannot easily be distinguished from the healthy pancreas *via* visual inspection and palpation during open surgery procedures [17]. Thus, traditionally, surgeons have determined the resection margin based on their experience through distal pancreatectomy with extended excision and resecting the specimen for frozen section analysis, which has low sensitivity for resection margins. Since these conventional methods do not improve patient outcomes, intraoperative real-time fluorescence imaging with an appropriate optical setup would allow for the surgeon to more objectively distinguish pancreatic tumors from normal tissues and achieve more accurate surgical resection.

Indeed, recent studies and clinical experience have shown that fluorescence technology can help to achieve submillimeter-sized precision when resecting micro-cancer tissues [18]. In the present study, the surgeon could sensitively recognize a tumor less than 4 mm in size with the guidance of optical imaging, which is too small to be detected with traditional imaging modalities. Such precise resection is not only essential for the prevention of tumor relapse but also helps to retain much more of the normal tissues, which is ultimately beneficial for normal physiological function to improve the survival and quality of life of patients with pancreatic cancer. Compared to extended distal pancreatectomy, we demonstrated that surgical navigation would improve the survival and quality of mice, as

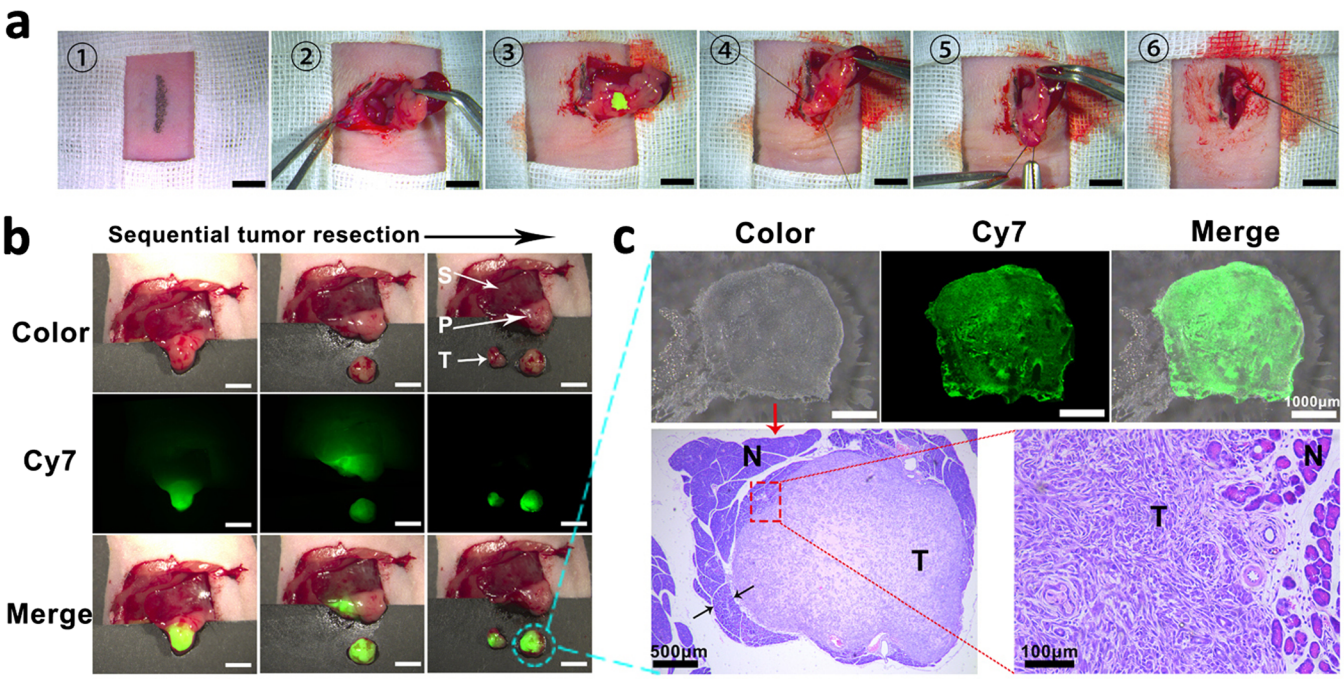

Fig. 5. Fluorescence-guided surgical resection. **a** Surgery of pancreatic tumor model guided by near-infrared fluorescence imaging at 6 h p.i. of peptide-22-Cy7. **b** Simulated resection *in vivo* would perform until no fluorescence was detected (scale bars = 3 mm). **c** Fluorescent imaging and subsequent pathological examination of tumor specimen. (Red dotted box represents tumor boundary; N = normal tissue; T = tumor; S = spleen; arrows respectively indicated tumor margin and outline of specimen in cross section).

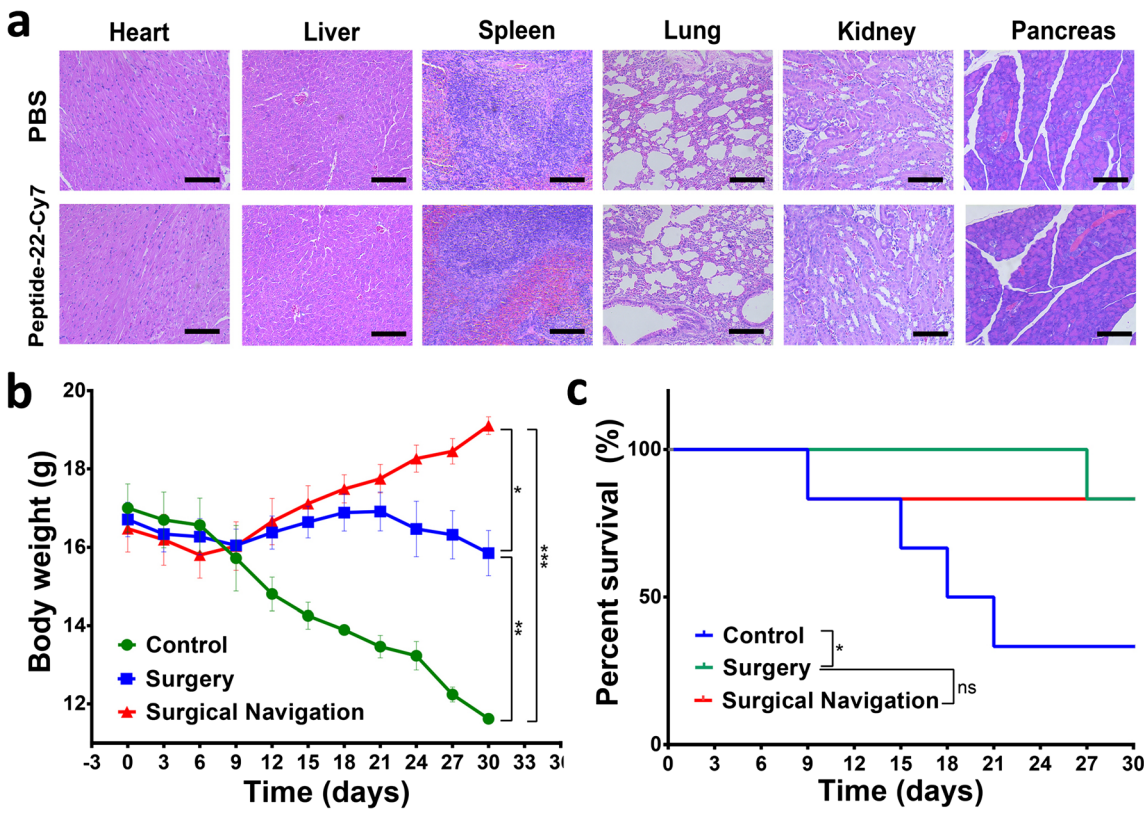

Fig. 6. Pathological test. **a** Major organs were collected for standard (H&E) staining. **b** Body weights of mice at post-treatment. **c** The mice survival after treatments. Scale bar = 500 μm.

manifested by the continuous increase in the body weights of the orthotopic mouse models. Moreover, since mortality was high in the control group, this highlights the importance of surgical treatment. Since late diagnosis will reduce the surgical opportunities, early screening of pancreatic cancer is essential to improve outcomes.

Photoacoustic imaging is an innovative non-invasive imaging technology based on a tunable and short pulsed laser at molecular absorption wavelengths to acquire an amplified acoustic wave. Compared with traditional imaging techniques, photoacoustic imaging can be used at bedside and is easily operated without radiation. Compared to ultrasonography, which was the first non-invasive imaging technique used to assess pancreatic malignancy, photoacoustic imaging shows higher tissue optical absorption contrast, which facilitates the early detection of pancreatic cancers [19]. As ultrasound signals are prone to weak scattering effects, the superiority of high spatial resolution and deeper penetration could achieve effective detection of accumulated probes in orthotopic pancreatic tumors while further complementing the deficiencies of NIR fluorescence imaging [20, 21]. In this experiment, photoacoustic imaging could detect a 4-mm pancreatic tumor *in situ*; although smaller tumors could also be detected with this technique in the nude mice, it was a bit more difficult owing to the impact of intestinal gas. Photoacoustic imaging still faces many challenges, including the depth of penetration, which has largely limited its clinical use: at present, the maximum photoacoustic imaging depth is 8.4 cm in chicken breast tissue [22]. To overcome this limitation, a large number of studies have focused on the effects of light scattering. Light could be focused in the scattering media through wavefront shaping [23], which could realize the imaging of organs far beneath the skin. When addressing all of these problems, photoacoustic imaging is expected to become one of the most important imaging methods for the early screening of localized small pancreatic adenocarcinoma in medical examinations.

Several biological targets of contrast agents have been extensively examined to achieve specific targeting. LDL is a routine factor assessed in clinical examinations, since its elevation is tightly linked to the development of cardiovascular events and diabetes, and it also plays an important role in lipoprotein metabolism. Glucose and glutamine are considered to be the key nutrients to sustain tumor growth. However, these nutrients are insufficient in the hypoxic environment of the tumor, including that of pancreatic cancer. Recent studies suggest that reprogramming lipid metabolism supports the rapid proliferation of tumor cells, especially by providing abundant cholesterol and fatty acids. Therefore, LDLR overexpression in pancreatic cancer cells is induced by increased cholesterol uptake during progression of pancreatic ductal adenocarcinoma (PDAC). Small hairpin RNA silencing of LDLR was shown to impede the proliferation of pancreatic tumor cells and limited activation of the ERK1/2 survival pathway [24, 25]. Moreover, in a previous study, the LDLR level was found to be 8.2 times higher in PDAC tissue compared with normal pancreatic tissue, suggesting LDLR as a potential therapeutic target [24]. In our study, we further verified that LDLR expression was higher in pancreatic cancer cells (PANC-1) than in normal pancreatic epithelial cells (HPDE6-C7) by western blot. There has been extensive research on LDL *in vitro* and a few of studies have intensively explored LDL as a nanovector for LDLR-targeting drug delivery, which could show high selectivity and safety to avoid clearance of the reticuloendothelial system. However, there are barely any studies on the application of LDLR in the imageology of pancreatic cancer. Numerous biomarkers that can specifically label pancreatic tumor cells have been explored [26], but few of these molecules have been tested in mouse models or in preclinical research. One problem with some of the highly expressed biomarkers in tumors is that they may be useful for one or two kinds of pancreatic cancer cell lines but are not applicable to all cell lines. As LDLR is overexpressed at all stages of pancreatic cancer and is widely distributed in all cancer cell lines, it is deemed to be a promising biological target for novel therapies. Furthermore, peptide-22 demonstrates high targeting ability towards LDLR and shows little competition with endogenous LDL.

In this study, we confirmed the targeting property of peptide-22-labeled dye from both cellular and animal experiments. In particular, both peptide-22-FITC and peptide-22-Cy7 showed specific targeting of the tumor area. Peptide-22-FITC was able to slowly penetrate though the vascular pores and enter tumor cells *via* receptor-mediated endocytosis, as the vasculature of the pancreatic tumor is either hypo-vascular or leaky. Owing to the physical barriers in pancreatic tumors, as well as the hypo-vascular property and interstitial hypertension, a highly specific probe with a small size (<50 nm in diameter [27]) is more suited for efficient permeability to pancreatic tumors as compared with larger nanoparticles. Furthermore, the small size of these probes has the advantage of expedited clearance. The relatively short-term period that the probe traveled throughout the body is an advantage for specific biomedical applications. Moreover, we observed some accumulation of peptide-22-Cy7 in the kidneys, which may be due to renal clearance of the small-molecule probes. The serum stability properties of peptide-22-Cy7 would further allow for increased accumulation at the tumor site so that sustained guidance could last for several hours to facilitate surgeries. Although some other emerging nanomaterials such as carbon nanotubes and quantum dots labeled with a peptide may also be used to acquire the same results, approval for these molecular probes is more difficult to obtain due to their long-term biotoxicity [28]. Therefore, a variety of NIR (650–900 nm) organic dyes such as indocyanine green, which are non-toxic and biodegradable, have been used for the development of contrast agents. Indeed, HE staining of the major organs of mice indicated the NIR dye Cy7 is non-toxic, which rules out its potential influence on the survival

and quality of the nude mice. Free indocyanine green cannot target pancreatic tumors, and because of its quenching characteristics, it is not suitable for straightforward conjugation to small peptides [29]. Therefore, Cy7 was selected for exploration in the present study. In addition, a slight red shift occurred after conjugation of Cy7 and peptide-22, which demonstrated the longer wavelengths to allow for deeper penetration into biological tissues, emitting weaker autofluorescence to the benefit of non-invasive fluorescence imaging [30]. *In vitro*, higher concentrations of peptide-22-Cy7 caused a certain degree of self-quenching, and much lower concentrations led to a weak fluorescence intensity, which would be unsuitable for optical imaging. Although a higher signal does not necessarily reflect a higher concentration of probes *in vitro*, the injection concentration of the fluorescence probe was relatively lower in the tumor tissue, which did not reach the self-quenching concentration *in vivo*.

This study has several limitations that should be mentioned. NIR imaging itself has certain limitations with regard to quantification, and photoacoustic imaging is insufficient for deep-tissue imaging in the human body. In addition, the probe of the pure dye-conjugated peptide is not sufficiently stable for long-term observation. Therefore, further breakthroughs in intraoperative imaging methods and developments of preoperative imaging equipment are needed. Moreover, further research effort should be devoted to contrast agents to meet clinical demands.

Nevertheless, this preliminary synthesis and assessment of peptide-22-Cy7 targeting PANC-1 human cancer cells support the potential clinical use of this probe. The superiority of its good biocompatibility, small size with no toxicity, and high specificity towards cancer cells *in vivo* may encourage the use of peptide-22-Cy7 for early screening and surgical navigation of pancreatic cancer. With further developments and optimization, these applications are expected to be tested in clinical studies in the near future towards improving the outcomes, diagnosis, and quality of life of pancreatic cancer patients.

Conclusion

The overexpression of LDLR on pancreatic cancer cells and its interactions with specific peptide-22 ligands were verified through *in vitro* and *in vivo* experiments. We used a high spatial resolution of photoacoustic tomography and the targeting property of peptide-22 to successfully detect a 4-mm orthotopic pancreatic tumor before surgery. We then investigated the potential of peptide-22-Cy7 in further application, which enabled the precise delineation of lesions from normal tissues by real-time intraoperative fluorescence imaging. As confirmed by histological examination, intraoperative precise resection was achieved with the fluorescence guidance of peptide-22-Cy7. The improvement of survival quality by surgical navigation was confirmed through the increased body weight and physical condition of mice.

The superior receptor targeting, fluorescence efficiency, small molecular size, non-radioactivity, and non-toxicity of this probe suggest that it has good potential to be used in broad clinical studies. With the development of novel equipment and probes for LDL-targeting, effective and simple-to-use multi-modality tomography will be applied to early cancer screening, and tumor targeting probes will greatly facilitate realizing precise imaging-guided surgery. Overall, these innovations are expected to lead to novel theranostic strategies for treating patients with pancreatic cancer.

Acknowledgements. The authors thank Tianpei Guan, Guanhua Lu, and Ting Ai for assistance with data collection.

Funding This work was supported by the National Natural Science Foundation of China under Grant Nos. 81227901, 81627805, 61231004, 61671449, 81501540, and 81527805; National Key R&D Program of China Grant under No. 2017YFA0205200; The Science and Technology Plan Project of Guangzhou (No. 201604020144); Digital Theranostic Equipment Research Special Program of The "13th five-year" National Key Research Plan (No. 2016YFC0106500); and The United Fund of National Natural Science Foundation of China and Government of Guangdong Province (Grant No. U1401254).

Compliance with Ethical Standards

Conflict of Interest

The authors declare no conflict of interest.

References

1. Kamisawa T, Wood LD, Itoi T, Takaori K (2016) Pancreatic cancer. Lancet 388:73–85
2. Michl P, Gress TM (2013) Current concepts and novel targets in advanced pancreatic cancer. Gut 62:317–326
3. Gillen S, Schuster T, Zum Buschenfelde CM et al (2010) Preoperative/neoadjuvant therapy in pancreatic cancer: a systematic review and meta-analysis of response and resection percentages. PLoS Med 7:e1000267
4. England CG, Hernandez R, Eddine SBZ, Cai W (2016) Molecular imaging of pancreatic cancer with antibodies. Mol Pharm 13:8–24
5. Dimastromatteo J, Brentnall T, Kelly KA (2017) Imaging in pancreatic disease. Nat Rev Gastroenterol Hepatol 14:97–109
6. McNally LR, Mezera M, Morgan DE et al (2016) Current and emerging clinical applications of multispectral optoacoustic tomography (MSOT) in oncology. Clin Cancer Res 22:3432–3439
7. Yan H, Zhao LY, Shang WT, Liu Z, Xie W, Qiang C, Xiong Z, Zhang R, Li B, Sun X, Kang F (2017) General synthesis of high-performing magneto-conjugated polymer core-shell nanoparticles for multifunctional theranostics. Nano Res 10:704–717
8. Hartwig W, Werner J, Jager D et al (2013) Improvement of surgical results for pancreatic cancer. Lancet Oncol 14:E476–E485
9. Nitschke P, Volk A, Welsch T, Hackl J, Reissfelder C, Rahbari M, Distler M, Saeger HD, Weitz J, Rahbari NN (2017) Impact of intraoperative re-resection to achieve R0 status on survival in patients with pancreatic cancer: a single-center experience with 483 patients. Ann Surg 265:1219–1225
10. Nguyen QT, Tsien RY (2013) Fluorescence-guided surgery with live molecular navigation—a new cutting edge. Nat Rev Cancer 13:653–662
11. Halbrook CJ, Lyssiotis CA (2017) Employing metabolism to improve the diagnosis and treatment of pancreatic cancer. Cancer Cell 31:5–19
12. Liu QP, Luo Q, Halim A, Song G (2017) Targeting lipid metabolism of cancer cells: a promising therapeutic strategy for cancer. Cancer Lett 401:39–45

13. Beloribi-Djefaflia S, Vasseur S, Guillaumond F (2016) Lipid metabolic reprogramming in cancer cells. Oncogene 5:e189. https://doi.org/10.1038/oncsis.2015.49
14. Huang JF, Li L, Lian JH, Schauer S, Vesely PW, Kratky D, Hoefler G, Lehner R (2016) Tumor-induced hyperlipidemia contributes to tumor growth. Cell Rep 15:336–348
15. Malcor JD, Payrot N, David M, Faucon A, Abouzid K, Jacquot G, Floquet N, Debarbieux F, Rougon G, Martinez J, Khrestchatisky M, Vlieghe P, Lisowski V (2012) Chemical optimization of new ligands of the low-density lipoprotein receptor as potential vectors for central nervous system targeting. J Med Chem 55:2227–2241
16. Zhang B, Sun XY, Mei H, Wang Y, Liao Z, Chen J, Zhang Q, Hu Y, Pang Z, Jiang X (2013) LDLR-mediated peptide-22-conjugated nanoparticles for dual-targeting therapy of brain glioma. Biomaterials 34:9171–9182
17. de Rooij T, Lu MZ, Steen W et al (2016) Minimally invasive versus open pancreatoduodenectomy systematic review and meta-analysis of comparative cohort and registry studies. Ann Surg 264:257–267
18. Chi C, Du Y, Ye J et al (2014) Intraoperative imaging-guided cancer surgery: from current fluorescence molecular imaging methods to future multi-modality imaging technology. Theranostics 4:1072–1084
19. Gerling M, Zhao Y, Nania S, Norberg KJ, Verbeke CS, Englert B, Kuiper RV, Bergström Å, Hassan M, Neesse A, Löhr JM, Heuchel RL (2014) Real-time assessment of tissue hypoxia in vivo with combined photoacoustics and high-frequency ultrasound. Theranostics 4:604–613
20. Taruttis A, Ntziachristos V (2015) Advances in real-time multispectral optoacoustic imaging and its applications. Nat Photonics 9:219–227
21. Sreejith S, Joseph J, Lin MJ, Menon NV, Borah P, Ng HJ, Loong YX, Kang Y, Yu SWK, Zhao Y (2015) Near-infrared squaraine dye encapsulated micelles for in vivo fluorescence and photoacoustic bimodal imaging. ACS Nano 9:5695–5704
22. Xia J, Yao JJ, Wang LV (2014) Photoacoustic tomography: principles and advances. Prog Electromagn Res 147:1–22
23. Lai PX, Wang LD, Tay JW, Wang LV (2015) Photoacoustically guided wavefront shaping for enhanced optical focusing in scattering media. Nat Photonics 9:126–132
24. Guillaumond F, Bidaut G, Ouaissi M, Servais S, Gouirand V, Olivares O, Lac S, Borge L, Roques J, Gayet O, Pinault M, Guimaraes C, Nigri J, Loncle C, Lavaut MN, Garcia S, Tailleux A, Staels B, Calvo E, Tomasini R, Iovanna JL, Vasseur S (2015) Cholesterol uptake disruption, in association with chemotherapy, is a promising combined metabolic therapy for pancreatic adenocarcinoma. Proc Natl Acad Sci U S A 112:2473–2478
25. Michalopoulou E, Bulusu V, Kamphorst JJ (2016) Metabolic scavenging by cancer cells: when the going gets tough, the tough keep eating. Br J Cancer 115:635–640
26. de Geus SWL, Boogerd LSF, Swijnenburg RJ, Mieog JSD, Tummers WSFJ, Prevoo HAJM, Sier CFM, Morreau H, Bonsing BA, van de Velde CJH, Vahrmeijer AL, Kuppen PJK (2016) Selecting tumor-specific molecular targets in pancreatic adenocarcinoma: paving the way for image-guided pancreatic surgery. Mol Imaging Biol 18:807–819
27. Adiseshaiah PP, Crist RM, Hook SS, McNeil SE (2016) Nanomedicine strategies to overcome the pathophysiological barriers of pancreatic cancer. Nat Rev Clin Oncol 13:750–765
28. Yang F, Jin C, Subedi S, Lee CL, Wang Q, Jiang Y, Li J, di Y, Fu D (2012) Emerging inorganic nanomaterials for pancreatic cancer diagnosis and treatment. Cancer Treat Rev 38:566–579
29. Lamberts LE, Koch M, de Jong JS, Adams ALL, Glatz J, Kranendonk MEG, Terwisscha van Scheltinga AGT, Jansen L, de Vries J, Lub-de Hooge MN, Schröder CP, Jorritsma-Smit A, Linssen MD, de Boer E, van der Vegt B, Nagengast WB, Elias SG, Oliveira S, Witkamp AJ, Mali WPTM, van der Wall E, van Diest PJ, de Vries EGE, Ntziachristos V, van Dam GM (2017) Tumor-specific uptake of fluorescent bevacizumab-IRDye800CW microdosing in patients with primary breast cancer: a phase I feasibility study. Clin Cancer Res 23:2730–2741
30. Liang XY, Shang WT, Chi CW, Zeng C, Wang K, Fang C, Chen Q, Liu H, Fan Y, Tian J (2016) Dye-conjugated single-walled carbon nanotubes induce photothermal therapy under the guidance of near-infrared imaging. Cancer Lett 383:243–249